



PORO-MECHANICAL COUPLING STRATEGIES FOR LARGE STRAIN COMPRESSION OF SOFT BIOLOGICAL TISSUES

José L. M. Thiesen¹, Bruno Klahr¹, Thiago A. Carniel², Eduardo A. Fancello¹

¹*Dept. of Mechanical Engineering, Federal University of Santa Catarina
Florianópolis, 88040-900, Santa Catarina, Brazil*

jose.thiesen@posgrad.ufsc.br, bruno.klahr@posgrad.ufsc.br, eduardo.fancello@ufsc.br

²*Polytechnical School, Community University of Chapecó Region
Chapecó, 89809-900, Santa Catarina, Brazil*

thiago.carniel@unochapeco.edu.br

Abstract. Early studies related to current poroelasticity theories are oriented towards problems in geomechanics. In addition to their use in soil mechanics, biphasic theories play an important role in the field of biological soft tissue mechanics. In this context, the elucidation of how mechanical stimuli are able to modify the behavior of cells within the tissue makes computational mechanics and mechanobiology extremely relevant fields. In general, due to the highly nonlinear coupled response coming from the biomechanical nature of the problem, large time-dependent deformations, damage, and fluid-structure interaction are complex behaviors that usually lead to difficulties in numerical solutions. Different types of schemes arise as an option to solve the mechanical equilibrium and mass conservation equations. Iteratively coupled methods emerge as an alternative to solve the biphasic problem. Therefore, in this paper, we propose a numerical investigation of the so-called *undrained* scheme applied to the finite element method using the updated Lagrangian approach. An unconfined case study is used to compare the response of the iteratively coupled method with the monolithic scheme, where the governing equations are solved simultaneously. In addition, the influence of an exponential permeability model on the volumetric strain and pore pressure fields is assessed.

Keywords: Poroelasticity, Iteratively-coupled schemes, Exponential permeability, Large deformation, Soft biological tissues

1 Introduction

The numerical treatment of poro-mechanical coupling has been widely addressed in the literature, especially in reservoir geomechanics [1–3]. Advances in numerical solution strategies for coupled problems can serve as a basis for the solution of the so-called biphasic problems applied to soft biological tissues. However, due to the assumptions used in the poroelastic problem for these tissues, the solution schemes in geomechanics are not always suitable for the biomechanics area. Since soft biological tissues are hypothesized to be a deformable porous media with incompressible constituents (solid and fluid), some solution strategies of biphasic problems can lead to numerical instabilities [1, 4].

The so-called staggered approaches, where each phenomenon is treated separately, is an alternative to solve biphasic problems [5, 6]. In this strategy, the exchange of information between the sub-problems occurs throughout hypotheses associated with the physics of the problem. These hypotheses characterize the different staggered solution methods presented in the literature. Among these methods, we focus here in the undrained split scheme, where the algorithm solves the mechanical problem ahead of the flow. This strategy is formulated by fixing the fluid mass content while solving the mechanical problem, leading to a pore pressure explicit update. In addition to these sequential schemes, the *monolithic* is also commonly used [7, 8]. In this method, the coupled equations are solved simultaneously at each time step generally by an implicit Newton-Raphson method. However, this scheme may result in linear systems that may require robust solvers and conditioning strategies [6].

Sequential strategies applied to finite element analysis under large deformations are not widely explored in

the literature, specially in the biomechanics context. In this paper, we propose a numerical investigation of the undrained scheme applied for the finite element method using the updated Lagrangian approach. An unconfined case study is used to compare the response of the iteratively coupled method with the monolithic scheme. The material parameters and specimen dimensions are set to represent the mechanical behavior of a biological tissue sample. This paper also aims to contribute to the investigation of the influence of a permeability model on the unconfined response. For this purpose, an exponential permeability rule was employed to assess the coupling level of the presented model.

2 Poroelasticity framework

2.1 Hypotheses

The mathematical description of a fluid flowing through a porous deformable media is accounted by poroelasticity formulations. Considering the mechanical characterization of soft biological tissues, the so-called biphasic models are established by assuming the following hypotheses:

1. No inertial or body force effects.
2. The process is quasi-static.
3. Fluid and solid constituents are assumed incompressible.
4. The porous media is fully saturated.
5. Additive decomposition of the total biphasic stress field into effective (constitutive model dependent of the solid skeleton strain) and hydrostatic (pore pressure dependent) parts.

2.2 Kinematical description

Let \mathcal{B}_0 indicate the undeformed Lagrangian configuration for the biphasic continuum media and let \mathbf{X}^α indicate the position of an α -constituent particle in the reference volume $\Omega_0^\alpha \subset \mathbb{R}^3$. The position of the particles \mathbf{X}^α in the current Eulerian configuration $\mathcal{B} = \Omega^\alpha \cup \partial\Omega^\alpha$ is given by

$$\mathbf{x}(\mathbf{X}^\alpha, t) = \mathbf{X}^\alpha + \mathbf{u}^\alpha(\mathbf{X}^\alpha, t), \quad (1)$$

where \mathbf{u}^α is the α -constituent displacement field. From this description, one can obtain all of the vector/tensor fields described from general continuum mechanics theory (*e.g.* deformation gradient, strain and stress tensors).

2.3 Solid skeleton constitutive model

In this study, the macroscopic material behavior of the solid skeleton is mathematically described by means of a hyperelastic constitutive law. The effective stress is derived from a scalar potential (stored strain energy function) called Helmholtz free energy function $\Psi = \Psi(\mathbf{C}^s)$. The material model used herein is the compressible isotropic neo-Hookean, whose stored strain energy is defined as

$$\Psi = \frac{\mu}{2}(I_1 - 3) - \mu \ln J^s + \frac{\lambda}{2}(\ln J^s)^2, \quad (2)$$

where $I_1 = \text{tr } \mathbf{C}^s$ indicates the first invariant of the right Cauchy-Green deformation tensor and J^s is the determinant of the solid skeleton deformation gradient \mathbf{F}^s . The second Piola-Kirchhoff stress tensor \mathbf{S}^s is derived through the partial derivative of Ψ with respect to the Green-Lagrange strain tensor \mathbf{E}^s ,

$$\mathbf{S}^s = 2 \frac{\partial \Psi(\mathbf{C}^s)}{\partial \mathbf{E}^s}, \quad \text{with} \quad \boldsymbol{\sigma}^s = \frac{1}{J^s} \mathbf{F}^s \mathbf{S}^s (\mathbf{F}^s)^T \quad (3)$$

2.4 Coupled equations

Recalling the aforementioned set of assumptions, the governing equations of a biphasic mixture are given by the overall equilibrium equation (Euler-Lagrange) and the continuity of mass. Thus, given the volume fractions ϕ^α , the permeability tensor $\boldsymbol{\kappa}$, the Lamé's parameters (λ, μ) , the constitutive model of the solid skeleton and a transport law for the fluid flow (Darcy's law), the problem is to find the fields of effective stress $\boldsymbol{\sigma}^s$, fluid relative

velocity \mathbf{w} , solid displacement \mathbf{u} and pore pressure p in such a way that

$$\operatorname{div} \boldsymbol{\sigma} = \mathbf{0}, \quad (4)$$

$$\boldsymbol{\sigma} = \boldsymbol{\sigma}^s + p\mathbf{I}, \quad (5)$$

$$\operatorname{div} (\mathbf{w} + \mathbf{v}^s) = 0, \quad (6)$$

$$\mathbf{w} = -\kappa \nabla p \quad (7)$$

are satisfied alongside with the Dirichlet and Neumann boundary conditions

$$\mathbf{u}^s = \bar{\mathbf{u}}^s \quad \text{on} \quad \partial\Omega_D^s, \quad (8)$$

$$\mathbf{t} = \boldsymbol{\sigma} \mathbf{n} = \bar{\mathbf{t}} \quad \text{on} \quad \partial\Omega_N^s, \quad (9)$$

$$p = \bar{p} \quad \text{on} \quad \partial\Omega_D^f, \quad (10)$$

$$q = \mathbf{w} \cdot \mathbf{n} = \bar{q} \quad \text{on} \quad \partial\Omega_N^f, \quad (11)$$

with \mathbf{n} being the outward normal of the current configuration, $\bar{\mathbf{t}}$ and \bar{q} the prescribed surface traction and flux on the Neumann boundaries $\partial\Omega_N^s$ and $\partial\Omega_N^f$, respectively.

2.5 Permeability model

Since the fluid flow through the porous media is modeled by Darcy's transport law, the linear relation between the relative velocity vector \mathbf{w} and the pore pressure gradient ∇p has to be established. Here, we employ the exponential isotropic permeability model, which states

$$\boldsymbol{\kappa} = \kappa(J^s)\mathbf{I}, \quad (12)$$

where

$$\kappa(J^s) = \kappa_0 \exp \left(M \frac{J^s - 1}{J^s - \phi_0^s} \right) \quad (13)$$

is a strain-dependent permeability parameter. In this model, κ_0 is the initial spatial permeability, M is an exponential constant that controls the nonlinearity level of the permeability with respect to the volumetric strain, and ϕ_0^s is the Lagrangian solidity [9].

3 Solution strategy

The solution of coupled poromechanical equations is widely investigated in the literature, especially in geomechanics [3, 4, 6]. However, instead of solving the mass balance and conservation of linear momentum equations simultaneously, it is common to adopt an iterative scheme integrated into a sequential strategy to solve the system of coupled equations. The former solution scheme is called monolithic, since it solves both equations in a fully-implicit way. The second is called iteratively-coupled (sequential), and is characterized by a splitting operator of the main problem.

In this work, we study the sequential strategy called undrained splitting scheme, where the mechanical balance is solved in front of the conservation of mass. The finite element method using an updated Lagrangian approach is used to solve both sub-problems. However, due to the distinct nature of both equations, one can use different discretization schemes. In order to compare the results of the undrained scheme, we also present a summary of the monolithic (fully-implicit) solution scheme.

3.1 Monolithic

As already stated, the monolithic (fully-implicit) scheme solves both equations (4) and (6) simultaneously. Thus, after linearizing the coupled equations and obtaining the desired system of equations, it is possible to use the Newton-Raphson method to obtain the primal solution variables \mathbf{u}^s and p . So, given a time partition $\Delta t = t_{n+1} - t_n$, the fully-implicit algorithm obtains the solution pair (\mathbf{u}^s, p) for each time increment after an appropriate convergence criteria. This scheme can be expressed as,

$$\begin{array}{c} \mathbf{u}^n \\ p^n \end{array} \Bigg| \xrightarrow{\mathcal{M}} \begin{array}{c} \mathbf{u}^{n+1} \\ p^{n+1} \end{array} \Bigg|, \quad \mathcal{M} : \begin{cases} \operatorname{div} \boldsymbol{\sigma} = \mathbf{0} \\ \operatorname{div} (\mathbf{v}^s + \mathbf{w}) = 0 \end{cases} \quad (14)$$

where the indices $(\cdot)^n$ and $(\cdot)^{n+1}$ represent the previous and current time stepping iteration, and \mathcal{M} indicates the monolithic operator. Although this method exhibits unconditional stability, its resulting system of equations is not symmetric. Furthermore, due to the distinct nature of each partial differential equation, the different orders of magnitude of the material parameters generally lead to ill-conditioned matrices.

3.2 Undrained

In this scheme, in addition to solving the mechanical balance equation before the mass conservation equation, a constraint on the fluid mass content is imposed under the balance equation. This constraint results in an explicit local prediction rule for the pore pressure within each finite element, yielding

$$p^* = {}^k p^{n+1} - \alpha({}^{k+1} \varepsilon_v^{n+1} - {}^k \varepsilon_v^{n+1}), \quad (15)$$

where ${}^k(\cdot)$ and ${}^{k+1}(\cdot)$ indicate the previous and current iteration of the sequential scheme, α is the undrained algorithm constant and ε_v is the volumetric deformation. After solving the mechanical problem, the fluid flow problem is handled with fixed geometry (no variation in the displacement field). Note that the pore pressure update must be taken into account in the linearization process of the weak-form equations, leading to additional terms in the Newton-Raphson tangent matrix.

The undrained iterative procedure can be expressed in a summarized form

$$\left| \begin{array}{c} {}^k \mathbf{u}^{n+1} \\ {}^k p^{n+1} \end{array} \right| \xrightarrow{\mathcal{U}_{mechanical}} \left| \begin{array}{c} {}^{k+1} \mathbf{u}^{n+1} \\ p^* \end{array} \right| \xrightarrow{\mathcal{U}_{flow}} \left| \begin{array}{c} {}^{k+1} \mathbf{u}^{n+1} \\ {}^{k+1} p^{n+1} \end{array} \right|, \quad (16)$$

$$(17)$$

with

$$\mathcal{U}_{mechanical} : \begin{cases} \operatorname{div} \boldsymbol{\sigma} = \mathbf{0} \\ \delta \dot{M}^f = 0 \end{cases} \quad \text{and} \quad \mathcal{U}_{flow} : \begin{cases} \operatorname{div} (\mathbf{v}^s + \mathbf{w}) = 0 \\ \delta \dot{\mathbf{u}} = \mathbf{0}, \end{cases} \quad (18)$$

where $\delta \dot{M}^f = 0$ represents the fluid mass content restriction and $\delta \dot{\mathbf{u}} = \mathbf{0}$ indicates that the geometry is kept fixed during the mass balance equation solution.

4 Unconfined compression finite element model

In order to investigate the nonlinear behavior of a soft biological tissue sample with respect to the exponential permeability model, a numerical case of unconfined compression was proposed (see Fig. 1 for the applied boundary conditions). In order to achieve a large deformation character, an axial compression (X_3 - direction) resulting in 20% of axial deformation was applied. As shown in Fig. 1, a controlled displacement of 4 mm/s was applied up to 0.4 mm. Then, the applied displacement was kept fixed until $t = 200$ seconds, in order to observe a relaxation behavior. To solve the coupled problem, the fully implicit and undrained schemes were used.

The unconfined compression was modeled with a three-dimensional mixed finite element mesh considering second-order Lagrange polynomials to interpolate the displacement field and first-order ones to interpolate the pore pressure field within the hexahedral element (U20P8 mixed element).

Regarding the constitutive behavior, this study employed a hyperelastic neo-Hookean material to represent the solid skeleton (Eq. (2)). The fluid flow through the porous domain was based on Darcy's law using the isotropic exponential permeability model (Eq. (13)). Table 1 presents all the parameters of the poroelastic material, the geometric characteristics and the time step considered in the analysis. A finite element mesh refinement was performed using five types of regular meshes: mesh 1 (18 elements), mesh 2 (96 elements), mesh 3 (408), mesh 4 (1040) and mesh 5 (2100). The mesh 4 was chosen, since the maximum relative error found for the radial displacement (X_1 direction) was 0.2%.

5 Results and discussions

To solve the biphasic problem, this study employed two different schemes: monolithic and undrained. While the monolithic one solves the system of nonlinear equations simultaneously, the undrained one solves the equations

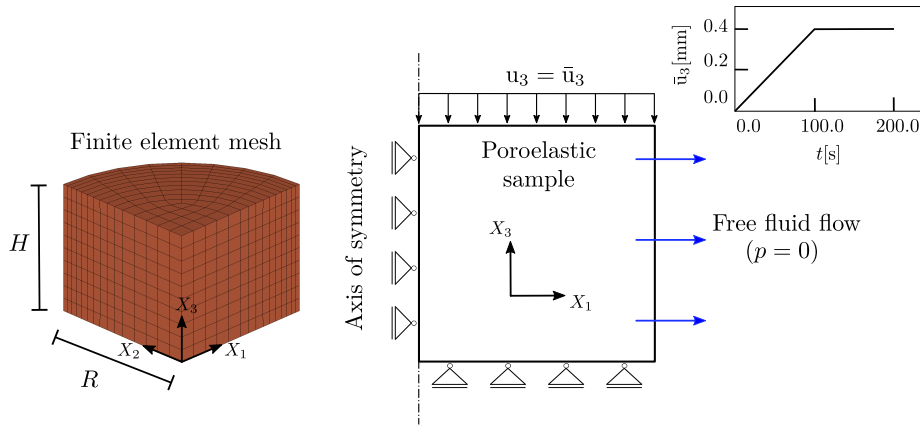


Figure 1. Finite element mesh and the applied boundary conditions for both displacement and pore pressure.

Table 1. Parameters used on the unconfined compression analysis.

Parameter	Unit	Value
First Lamé's, λ	MPa	15.0
Shear modulus, μ	MPa	10.0
Hydraulic permeability, κ_0	mm ⁴ /Ns	0.01
Exponential constant, M	-	0.5 - 4.0
Solidity, ϕ_0^s	-	0.3
Height, H	mm	2.0
Radius, R	mm	2.0
Time step, Δt	s	2.0

sequentially, within an iterative process for each time step. Despite the distinct way of solving the coupled problem, both solutions of the schemes are expected to converge to the same results. Fig. 2 presents the pore pressure and volumetric Jacobian using these strategies. It can be seen that the iteratively coupled scheme is able to achieve the same results as those obtained by the monolithic method.

In addition to presenting coupled solution strategies to the biphasic problem, this paper also aims to investigate the effect of varying the parameters of the permeability model on the results of the numerical case of unconfined compression. For this purpose, a strain-dependent permeability model (Eq. (13)) was used. It can be seen that the larger the parameter M , the more the permeability decreases with increasing compressive strain. This behavior is seen in experimental studies of soft biological tissues [10, 11].

Figure 2a-b shows the pore pressure obtained for the unconfined compression case. To investigate the influence of the permeability model, different exponential parameters M were tested. It can be seen that higher values of M increase the fluid flow resistance, which can be verified due to higher values of pressures and pressure gradients. It can also be seen that the increase of M also increases the sensitivity of pore pressure values with a variation of the permeability model parameter. On the other hand, it is found that the variation of the parameter M has a minor influence on the volumetric Jacobian. Figure 2c-d presents the curves obtained for the volumetric Jacobian. Although the response of the volumetric Jacobian over time has a small variation with M , Fig. 2d shows that with an increase in the value of M , the greater is the gradient of the volumetric strains.

It can be seen that high values of M result in a sudden decrease in permeability values with deformation, and this directly influences the coupling level of the analysis. Afterwards, in cases of large volumetric deformations, higher values of M can lead to convergence problems within the numerical solution process.

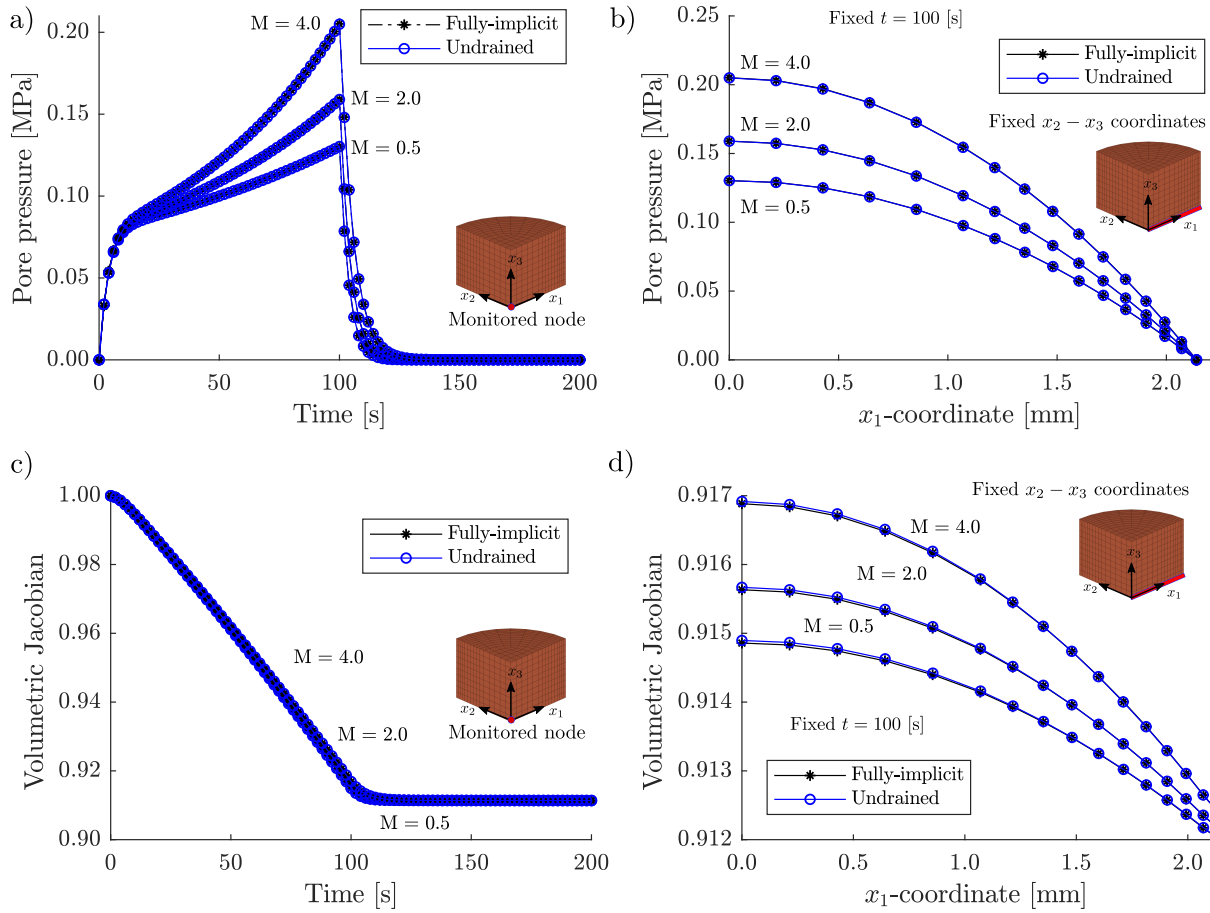


Figure 2. Pore pressure and volumetric Jacobian values as functions of time and spatial x_1 - coordinate using three representative values of exponential parameter M .

6 Final remarks

This paper presented a numerical investigation of the undrained splitting scheme to solve a finite-strain poroelasticity problem applied to soft biological tissues, in particular, a case of compression of an unconfined specimen. Since connective tissues such as tendons, cartilage, and intervertebral discs are poorly vascularized structures, it is common to model them as a biphasic body with a low hydraulic permeability to investigate the fluid flow characteristics in their interior. The permeability parameter plays an important role in the coupling strength of biphasic models and, consequently, directly influences the convergence of the computational solution schemes. We performed an investigation of the undrained scheme for solving an unconfined compression case. For this purpose, a three-dimensional finite element model was developed.

So as to evaluate the influence of permeability on the problem under consideration, a strain-dependent permeability model is considered in the analysis. From the results obtained, it was possible to verify that the undrained iterative scheme produced the same results as those obtained by the monolithic approach. Although the permeability model parameter M had an influence on the pore pressure results, it had a small impact on the response of the volumetric Jacobian under the applied kinematic constraints.

Acknowledgements. The authors would like to thank the following funding agencies: CAPES - (Coordination for the Improvement 426 of Higher Education Personnel) and CNPq - (National Council for Scientific and Technological Development).

Authorship statement. The authors hereby confirm that they are the sole liable persons responsible for the authorship of this work, and that all material that has been herein included as part of the present paper is either the

property (and authorship) of the authors, or has the permission of the owners to be included here.

References

- [1] J. Kim, H. A. Tchelepi, and R. Juanes. Stability, accuracy, and efficiency of sequential methods for coupled flow and geomechanics. *SPE Journal*, vol. 16, n. 02, pp. 249–262, 2011.
- [2] M. R. Correa and M. A. Murad. A new sequential method for three-phase immiscible flow in poroelastic media. *Journal of Computational Physics*, vol. 373, pp. 493–532, 2018.
- [3] J. Kim. A new numerically stable sequential algorithm for coupled finite-strain elastoplastic geomechanics and flow. *Computer Methods in Applied Mechanics and Engineering*, vol. 335, pp. 538–562, 2018.
- [4] F. Armero. Formulation and finite element implementation of a multiplicative model of coupled poro-plasticity at finite strains under fully saturated conditions. *Computer Methods in Applied Mechanics and Engineering*, vol. 171, n. 3-4, pp. 205–241, 1999.
- [5] M. Vaz and M. Lange. Thermo-mechanical coupling strategies in elastic–plastic problems. *Continuum Mechanics and Thermodynamics*, vol. 29, n. 2, pp. 373–383, 2017.
- [6] O. Duran, M. Sanei, P. R. Devloo, and E. S. Santos. *An enhanced sequential fully implicit scheme for reservoir geomechanics*, volume 24. Computational Geosciences, 2020.
- [7] M. Levenston, E. Frank, and A. Grodzinsky. Variationally derived 3-field finite element formulations for quasistatic poroelastic analysis of hydrated biological tissues. *Computer Methods in Applied Mechanics and Engineering*, vol. 156, n. 1-4, pp. 231–246, 1998.
- [8] S. Hirabayashi and M. Iwamoto. Finite element analysis of biological soft tissue surrounded by a deformable membrane that controls transmembrane flow. *Theoretical Biology and Medical Modelling*, vol. 15, n. 1, pp. 21, 2018.
- [9] G. A. Ateshian and J. A. Weiss. Anisotropic hydraulic permeability under finite deformation. *Journal of biomechanical engineering*, vol. 132, n. 11, 2010.
- [10] V. C. Mow and J. M. Mansour. The nonlinear interaction between cartilage deformation and interstitial fluid flow. *Journal of biomechanics*, vol. 10, n. 1, pp. 31–39, 1977.
- [11] F. Boschetti, G. Pennati, F. Gervaso, G. M. Peretti, and G. Dubini. Biomechanical properties of human articular cartilage under compressive loads. *Biorheology*, vol. 41, n. 3-4, pp. 159–166, 2004.